Scientific/Technical/Management Section

1 Introduction

The understanding of magnetic reconnection at the magnetopause and its impact on the Earth's magnetosphere is a fundamental research area of space plasma physics. This process is one of the most important for coupling energy, mass, and momentum from the solar wind into the Earth's magnetosphere. It is now clear that, rather than the closed magnetosphere models proposed in the early years of space physics research, the open magnetosphere model of *Dungey* [1963] is the correct view. Nonetheless, there remain significant questions as to the character of plasma entry at the Earth's cusps. In particular, the question of whether the reconnection process is temporally sporadic from a fixed spatial location or temporally steady from a variety of spatial locations remains unresolved and is the focus of this proposal.

The Earth's cusp provides a unique laboratory in which to test these two models of the reconnection process. Assuming steady IMF B_Z southward solar wind conditions, the field lines which have been recently opened through reconnection first link to the cusp ionosphere as they convect in the anti-sunward direction over the polar cap. In the case of steady reconnection at a fixed X-point, the ions which cross the magnetopause just as the field line is reconnected have higher average energies than those which cross the magnetopause as the field line gradually unkinks as it convects anti-sunward. This, combined with time-of-flight velocity filter effects, leads to a characteristic energy-time dispersion signature within the cusp in which the highest energy ions arrive at the most equatorward position within the cusp with decreasing energy as latitude increases in the poleward direction [*Onsager et al.*, 1993].

However, this simple picture of continuous dispersion is frequently not observed. Instead, discontinuous changes in energy are observed which give the appearance of steps in the dispersion signature *Newell and Meng* [1991]. These steps have been interpreted in one of two ways, either temporal variation in the reconnection rate [*Lockwood and Smith*, 1989; *Lockwood and Smith*, 1994] or as steady reconnection from multiple X-points [*Lockwood and Smith*, 1992; *Onsager et al.*, 1995]. The controversy over these two models is not yet resolved. Studies that combine cusp observations from DE, Interball-AP, Polar and Fast [e.g., *Onsager et al.*, 1995; *Trattner et al.*, 1999, 2002] point to the multiple X-point model whereas other work [e.g., *Escoubet et al.*, 1992, 2006; *Boudouridis et al.*, 2001; *Lockwood et al.*, 2001] argues for the temporally varying reconnection model. Similarly, spatial or temporal structure was not resolved by mapping cusp structures observed by the Cluster satellites along the geomagnetic field lines to the ionosphere and combining them with SuperDARN radar observations [e.g., *Trattner et al.*, 2003, 2005a]. Spatial and temporal cusp structures have also been reconstructed and discussed by *Connor et al.* [2012], who used test particles with a 3D global MHD model. One way to distinguish between these two views is by comparing measurements from two spacecraft which traverse the cusp region at different times. Such comparisons have been made, but typically the spacecraft are separated by relatively large differences in either space or time such that the results are not conclusive [*Trattner et al.*, 2002]. To detect spatial cusp structures the observer needs to cross the boundary between multiple reconnection lines. However, each of these structures can also be dominated by temporal effects. Spatial cusp structures will be encountered at the same latitude while temporal cusp structures will move to different locations as shown in Figure 1, discussed below. By coordinating the launches of two very similarly instrument sounding rockets; we will make measurements which will be sufficiently close in time and space to resolve the differences between these two models.

In addition to signatures of the more global issue of the temporal/spatial variation of reconnection, the magnetosphere-ionosphere connection through the cusp introduces a host of electrodynamic phenomena with both local and global coupling implications. These phenomena include field-aligned

currents and ion heating associated with the open/closed field boundary in the cusp. These currents may be carried by precipitating electrons in the form of poleward moving auroral forms that are thought to be associated with the steps in ion energy dispersion [*Fasel*, 1995; *Lockwood et al.*, 2001]. Our measurement suite will reveal the electrodynamics of the cusp/boundary layer in the upper ionosphere with outstanding, meter-scale resolution. In particular, we will characterize the transition from open to closed field lines, using energetic particle and plasma wave data to mark the transition. By comparing high-flying and low-flying payloads, we will investigate current closure in the cusp region including the role of Poynting flux and Alfvén waves in accelerating electrons that may carry these currents.

The proposed TRICE-2 mission is a reflight of the TRICE mission, appropriately modified to eliminate the failures on the first mission. While the TRICE rockets returned significant scientific data on the electrodynamics of the cusp [*Li et al.*, 2010; *LaBelle et al.*, 2010; *Dombrowski et al.*, 2012], the ion and electron instruments failed and no data were returned on the primary objective to understand the stability of cusp reconnection. The cause of the failures have since been rectified through improved design and parts selection and have been demonstrated to work in multiple spaceflight experiments. The primary science objective of the TRICE mission remains unanswered, but will be answered by TRICE-2.

For the TRICE-2 reflight, we will launch a pair of almost identically instrumented scientific payloads from Norway's Andoya Rocket Range into the Earth's cusp region during a period when optical data show the presence of poleward moving auroral forms and radar data indicate that significant ionospheric signatures of reconnection are present. The two rockets will fly along very similar ground tracks, but one will fly to an apogee of approximately 500 km and the other will fly to an apogee of ≥ 1200 km. This two rocket launch was successfully accomplished for the original TRICE mission. By launching the low-flying rocket after the high-flying rocket, we will achieve a variety of separations across magnetic field lines between the payloads in both the north-south and east-west directions as well a separation in the times at which the payloads traverse a given magnetic latitude. This will allow us to separate space and time variation along the rocket tracks as well as some separation across the rocket tracks.

Identical instruments on the two payloads will provide measurements of the high frequency electric field waveforms, high-time-resolution electron distributions, ion distributions, low frequency waves, DC-electric fields, and the electron density. The instruments are all tested designs with flight heritage most recently from the ACES, CHARM-2, and GREECE rockets and the Juno and Van Allen Probes satellites. The novel aspect of this experiment lies in the ability to place a pair of rockets into the topside ionosphere of the cusp with a separation of space and time both along the magnetic field and across the magnetic field. This will allow us to gather simultaneous data at two altitudes and to exploit the inherent ability to resolve spatial and temporal variations afforded by two payloads with different trajectories. In particular, this will allow us to directly test the predicted in-situ ionospheric signatures of 'pulsed' reconnection and compare these measurements with those of ground-based instrumentation by examining the evolution of cusp ion dispersion as a function of latitude at a variety of different times. In addition, our comprehensive suite of measurements will allow a detailed study of the temporal and spatial evolution of the electrodynamics and particle precipitation in the cusp. These measurements will be compared with simultaneous ground-based measurements from radar and imaging detectors. The experiment will answer significant questions concerning the temporal evolution of cusp reconnection and electrodynamic signatures and will provide "space truth" for interpreting ground-level measurements of the cusp region.

TRICE-2 Key Features

- Overarching goal: Determine whether cusp dynamic structures are the result of temporal or spatial variation in magnetopause reconnection

- Two nearly identically instrumented rockets flying at low and high altitudes with a variety of separations in time and space
- Simultaneous ground-based measurements confirming signatures of reconnection in the cusp and providing global context of the ionospheric electrodynamics.

2 Proposed Twin Rocket Investigation of Cusp Electrodynamics 2: Science Rationale

The primary goal of the proposed rocket mission is to measure cusp signatures of reconnection occurring at the magnetopause during steady IMF B_Z southward conditions. Due to the time separation of the two payloads along essentially the same set of magnetic coordinates, we will be able to distinguish signatures of pulsed reconnection and those of steady reconnection with varying X-points. At the same time we will compare the in situ measurements with ground-based measurements from the EISCAT and SuperDARN radars as well as with optical measurements made from Svalbard, Norway. The cusp is often thought of as a dayside feature, but during the northern hemisphere's winter season, the cusp's ionospheric footpoint is often in darkness and directly over Svalbard. This enables the use of optical imaging for cusp studies. providing visual confirmation of a key signature of cusp activity, the poleward moving auroral form (PMAF).

By flying two essentially identically instrumented payloads through the cusp with varying time separation, we will be able to answer the following questions:

- **Is the signature of pulsed reconnection observed? That is, have steps in dispersed ion energy signature propagated poleward by the amount expected from convection for the time difference between observations at the same invariant latitude?**
- **Is the signature of multiple, stationary X-points observed? That is, are the steps in ion energy dispersion fixed in invariant latitude?**
- **Is the signature of electron precipitation always observed at steps in the ion energy dispersion and does this show evidence of field-aligned currents?**

While association of the cusp with reconnection is beyond dispute, the nature of the reconnection remains controversial. The apparent continuous nature of the particle precipitation and enhanced electron temperatures associated with the cusp do not imply that the reconnection is continuous, as explained in a review by [*Smith and Lockwood*, 1996]. Indeed, modeling of low-altitude signatures of pulsed time-dependent cusp reconnection is well developed and the subject of numerous papers (see for example, *Lockwood et al.* [2001] and references therein). One consequence of this model is the existence of ion "steps." As described above, for IMF $B_Z < 0$, ions are dispersed as they travel down the field line from the X-point, implying that the highest energy ions reach the ionosphere equatorward of the slower ions. There are two reasons for this: first, the standard velocity filter effect implies that higher energy ions will be observed along the most recently reconnected field line, meaning the most equatorward one in the context of the cusp, while lower energy ions will be observed along field lines poleward of that which were actively reconnecting further in the past. Second, if the reconnected flux is eroding the magnetosphere, implying that the reconnection point is shifting equatorward as magnetic flux is stripped away, this reinforces the velocity filter effect.

How a given spacecraft observes the dispersion, i.e., whether it detects high energy ions first and later low energy ions, or vice versa, depends on how the satellite north-south velocity compares with the

north-south convection of the field lines; a satellite traveling faster than the convection (overtaking the convection) will see a reversed feature versus one traveling slower than the convection. Satellite observations at high and low altitudes confirm this velocity dispersion feature in cusp ions, but significantly, interruptions or "steps" in the pattern commonly occur multiple times during cusp crossings [*Lockwood and Smith*, 1989; *Newell and Meng*, 1991; *Escoubet et al.*, 1992].

The pulsed reconnection model predicts such ion steps; the individual ion steps correspond to separate episodes of reconnection. Examining satellite ion data in light of the model allows inversion of observed ion "steps" to obtain reconnection patterns. As reviewed by *Smith and Lockwood* [1996], applying such inversion to satellite crossings of the cusp implies the reconnection is highly pulsed, even when the precipitation seems steady-state. In many cases, for example those published by *Newell and Meng* [1991], the reconnection rate fluctuates but seldom if ever goes to zero. In other cases, the model applied to ion data implies that reconnection turns on and off. Recently, *Lockwood et al.* [2001] worked out the consequences of the pulsed reconnection model for the signs of field-aligned currents at the cusp ion step boundaries and found these predictions consistent with Polar satellite data.

Other evidence for pulsed time-dependent reconnection dominating the cusp revolves around simultaneous satellite-ground based data, specifically the identification of cusp ions steps with Poleward moving auroral forms (PMAFs) [*Yeoman et al.*, 1997; *Farrugia et al.*, 1998], or with boundaries of longitudinal flow features in radar data, which are in turn associated with features in global UV images [e.g., *Milan et al.*, 2000]. The large local time extent of the last feature speaks to the possible significance of pulsed reconnection to magnetospheric physics, since if the interpretation is correct it implies that almost all of the magnetospheric flux transfer would be explained by these events.

However, pulsed or time-variable reconnection is not the only explanation for the ion "steps" observed in the cusp. These features would also be expected from stationary reconnection features spatially separated, along the field lines penetrated by a spacecraft. The difference between the two pictures, spatial or temporal variation, is illustrated in Figure 1 taken from *Trattner et al.* [2002]. This figure shows the difference in the signatures seen by two spacecraft that would be expected for pulsed reconnection (left hand side) and spatially varying, steady reconnection (right hand side). In each case, Spacecraft 2 traverses the cusp in the poleward direction before Spacecraft 1. For spatial variation, the pattern of reconnection is fixed and both spacecraft see the same features at the same latitude. For pulsed reconnection, the steps in the dispersion signature convect poleward with time and hence the pattern seen by Spacecraft 1 at a later time is shifted poleward.

Indeed, despite the large body of evidence cited above for time-dependent reconnection dominating the cusp, dual spacecraft measurements have been reported which tend to support the spatial interpretation of the reconnection features. For example, *Onsager et al.* [1995] examine ion step features observed nearly simultaneously in the cusp with DE-1 and DE-2 and conclude that their case study corresponds to a stationary feature. Similarly, *Trattner et al.* [1999] report cusp features at the same location in satellite crossings 1.5 hrs apart. *Trattner et al.* [2002] confirmed this result with statistics of cusp crossings by Polar at high altitudes and FAST at low altitudes, finding that statistically these satellites encounter the same number of cusp steps per crossing even though Polar takes ten times longer to cross the cusp than does FAST. This result appears consistent with a spatial interpretation. Pulsed reconnection would appear to imply that the satellite which takes more time should see more events. The satellites also see similar ion signatures even though one has velocity smaller than the convection of the field lines, and the other has velocity which exceeds convection, a signature likewise consistent with the spatial interpretation of the ions step features. *Trattner et al.* [2002] also observed that, statistically, the ion step boundaries occur at the same latitudes for similar solar wind conditions, which implies they are at fixed locations determined by the conditions and may contradict the pulsed reconnection model. Nonethe-

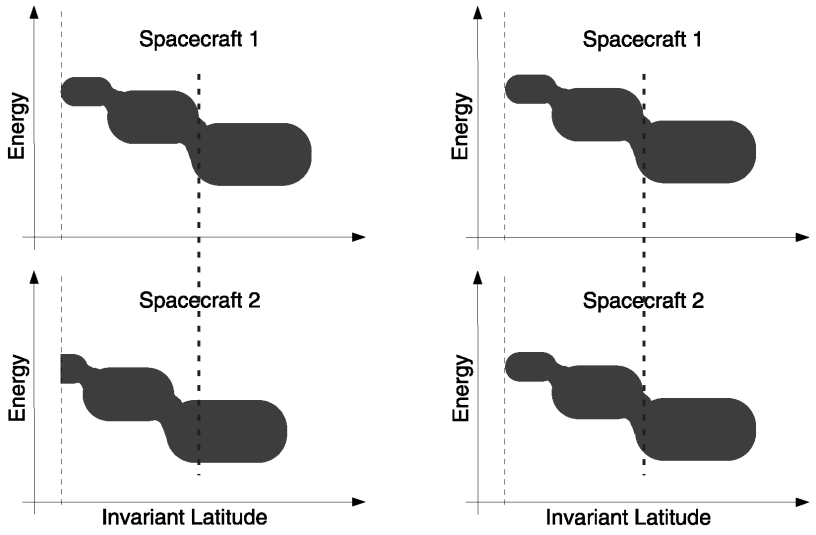

Figure 1: A comparison of the signatures seen by two spacecraft for pulsed reconnection (left hand side) and spatially varying, steady reconnection (right hand side). In each case, Spacecraft 2 traverses the cusp in the poleward direction before Spacecraft 1. For pulsed reconnection, the steps in the dispersion signature convect poleward with time and hence the pattern seen by Spacecraft 1 at a later time is shifted poleward. For spatial variation, the pattern of reconnection is fixed and both spacecraft see the same features at the same latitude. The TRICE-2 rockets distinguish between these two possibilities and therefore determine whether reconnection is pulsed or spatially varying.

less, even *Trattner et al.* [2002] say that some of the features that they observed could be explained as temporal variation in the reconnection rate.

Further ambiguous evidence was presented by combining Cluster cusp observations with simultaneous observations of the ionospheric convection pattern provided by the SuperDARN radar array [*Trattner et al.*, 2005b]. Cluster cusp structures were mapped to the ionosphere along geomagnetic field lines and their location plotted with respect to the ionospheric convection cells. The cusp structures can be described as spatial features observed by satellites crossing into spatially separated flux tubes, but they can also be observed as poleward-traveling (temporal) features within the same convection cell, most probably caused by variations in the reconnection rate at the magnetopause.

In summary, the nature of the predominant means of cusp reconnection remains a major unsolved problem, despite a significant number of sophisticated theoretical, modeling, and experimental approaches to the problem. Distinguishing spatial versus temporal interpretations requires simultaneous observations at two points in space. While the dual satellite observations, DE-1 and -2 or Polar/FAST, have been valuable and have the advantage of plumbing a wide range of altitudes as described by *Trattner et al.* [2002], the dual rocket observations proposed here offer complementary advantages. Principally, it is easy to achieve closer separation of the spacecraft in time and space, and that separation can be variable during a cusp crossing which is very valuable for checking the results. In addition, the rockets provide significant time within the cusp due to lower velocity as compared with satellites. As an example of rocket measurements in the cusp, Figure 2 shows the electron precipitation data from the SCIFER payload [*Lorentzen et al.*, 1996]. At 700 s, the rocket crossed from closed to open field lines as demarcated by the end of the trapped electrons above 1 keV. The payload continued to see cusp electrons for another 600 s. This rocket flew a very similar trajectory to that of the proposed high-flyer

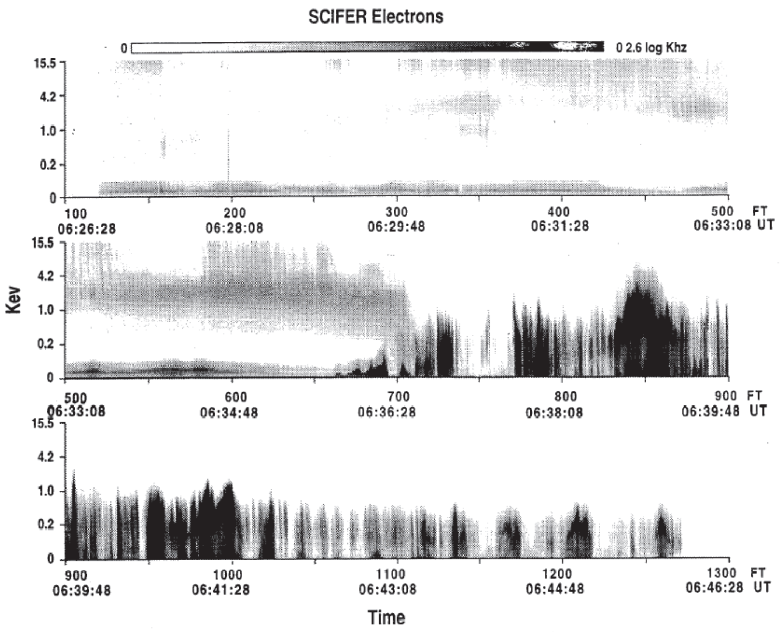

Figure 2: Full-flight electron measurements from the SCIFER rocket from *Lorentzen et al.* [1996]. This rocket followed a very similar trajectory to that proposed for the TRICE high-flyer payload. The rocket entered the cusp at around 700 s when the low energy electrons are observed. The high-flying TRICE-2 rocket will make similar measurements for 600 s in the cusp and, combined with the ion measurements, determine whether reconnection is temporally or spatially varying.

and shows that we will have ample flight time within the cusp. The low-flyer has a shorter flight time, but will be within the cusp for approximately 300 s.

The north-south rocket velocity of about 1 km/s is comparable to the convection velocity, possibly introducing some additional complexity in identifying ion dispersion signals, but also providing an additional method of distinguishing the temporal from spatially stationary interpretations. The essential difference between the interpretations comes from measuring the locations of the ion step features observed by the two rockets and noting whether they are stationary or convecting. The rockets will encounter the same spatial region with a time difference varying from about -100 s to +100 s during the cusp crossing. This temporal difference is large enough for convection to move the ion steps a significant distance, but small enough that flux erosion, which moves the overall position of the cusp, is not a large effect. If the features move at, for example, the convection speed of a reconnected field line which is 0.5-1 km/s, this would correspond to up to a 50-100 km spatial displacement, easily detectable, and the reduction of that displacement as the rocket spacing changes and reverses is likewise easily observable. In fact, TRICE-2 will easily detect displacements of convecting features moving with less than 10% of the typical convection velocity, ensuring the ability to discern moving forms from stationary forms.

High-time resolution electron measurements on the rockets, with high data rates as allowed by rockets, will provide additional diagnostics of the cusp features, since the boundaries of the ion steps are characterized by electrons. The timing of these electron bursts, relative to the dispersed ions, allow an estimate of the distance to the reconnection site due to the time-of-flight difference between species. High resolution wave data, including waveforms with frequency response exceeding the plasma frequency, again possible because of high rocket telemetry rates, can be useful as a surrogate for particle features, as was the case for example during Viking cusp crossings at higher altitude, where electron

acoustic wave bursts served as indicators of electron bursts, and the timing between these and dispersed ions provided an estimate of the distance to the reconnection site [*Pottelette and Treumann*, 1998]. In addition, magnetometers on both rockets will measure the locations and signs of field-aligned currents relative to cusp ion steps, enabling a further detailed test of the pulsed reconnection model along the lines of that performed by *Lockwood et al.* [2001] using Polar data.

Finally, it is worth noting that the location of the reconnection region remains an outstanding and significant mystery. Observations suggest that the X-line is extended in longitude, for example, *Peterson et al.* [1998] using FAST and Polar data; *Phan et al.* [2000] using GEOTAIL and WIND observations with the two satellites spaced in local time on either side of the equator; and the evidence based on associating forms in global UV images with pulsed reconnection events described above [*Milan et al.*, 2000]. Long but not necessarily continuous reconnection lines have also been observed by the IMAGE satellite which showed that both reconnection scenarios, anti-parallel and component reconnection, occur at the magnetopause for southward IMF conditions [*Fuselier et al.*, 2002a; *Fuselier et al.*, 2003].

Polar and Cluster observations of precipitating and mirrored ion distributions in the cusp have been used to determine the distance to the reconnection line at the magnetopause by comparing the difference in velocity cutoff between downward and upward (reflected) populations. This led to the development of the Maximum Magnetic Shear model [e.g., *Trattner et al.*, 2007]. The distance to the reconnection site determined by this technique can be used to distinguish between temporal and spatial cusp structures. It has been shown that spatial cusp structures have reconnection sites located in different hemispheres [*Trattner et al.*, 2005a] while temporal cusp structures map to the same location along the Line of Maximum Magnetic Shear [*Trattner et al.*, 2008]. Despite this evidence, the question is far from decided, and is of great significance since it determines effectively how much flux transfer can be accounted for by cusp reconnection events. The low altitude of the rockets compared to satellites such as Polar and FAST will decrease the velocity separation between the precipitating and mirrored ion beams, but the higher time resolution and good pitch angle resolution of the rocket measurements will mitigate this. This technique augments the primary methodology of observing variations in the ion step features.

The second major science goal is to compare the electrodynamic signatures of poleward moving auroral forms at two altitudes in order to better determine the electric field, particle precipitation and current structure of these auroral features. Two payloads, one flying high and one flying low will allow us to investigate the variation in altitude of field line currents, electric fields and particle energization to address the following questions:

- **How does parallel current in the cusp vary with altitude and what role do transversely accelerated ions and electrons play in carrying this current? What is the relation of Poynting flux to these charge carriers? Is Poynting flux dissipated as a function of altitude in the ionosphere?**
- **Do Alfvén waves play a significant role in poleward moving auroral forms? Do Alfvén waves represent the signature of newly opened magnetic field lines?**
- **Which wave modes characterize the cusp ionosphere? How do these differ from those observed at mid-altitudes by Viking and Polar? Can wave observations be used as proxies for the presence of electron beams or currents?**

Electron measurements on each of the rockets will delineate the boundary of the trapped electrons with energies $\geq$ 1 keV, as on SCIFER (see Figure 2), determining the boundary between open and closed field lines. This information is valuable for a host of studies, for example, resolution of the controversy concerning the location of cusp field-aligned currents relative to this boundary. From statistical analysis

of the latitude dependence of the cusp field-aligned currents measured with the magnetometers on the Oersted satellite under conditions of large IMF B_Y, *Stauning et al.* [2001] found that the field-aligned currents lie along closed field lines, a conclusion confirmed with case studies in which electron data from the satellite could be used to identify the closed-open boundary. However, *Sandholt et al.* [2002] reached opposite conclusions from analysis of the field-aligned currents occurring during DMSP crossings of the cusp under strongly negative IMF B_Y conditions. *Strangeway et al.* [2000] reviewed models of field-aligned currents in the cusp under different IMF B_Y conditions (see their Figure 4a-c). The FAST data they analyzed, during an interval of large IMF B_Y, suggested that most of the cusp region field-aligned currents are along open field lines. Although we plan to avoid large IMF B_Y conditions in launching TRICE, IMF B_Y will likely exceed a few nT, implying a current system will be set up along the lines described in Strangeway et al [2000], in which case TRICE-2 will directly determine on which side of the open/closed boundary that the field-aligned currents occur.

The SCIFER mission found that transverse ion acceleration was associated with field-aligned currents of up to 20 μA/m^2 [*Kintner et al.*, 1996]. A more recent study by *Strangeway et al.* [2000] found that these field-aligned currents in the cusp are driven by the reconnection process and that these currents are present for all orientations of the IMF. This work showed that the orientation of the currents depends on the IMF B_Y component. The authors argued that stresses caused by shearing in the coupling between the magnetopause and cusp ionosphere sets up these currents as a necessary means of overcoming the drag force on these field lines presented by the ionosphere. With our dual payloads at differing altitudes, we will be able to measure differences between the field-aligned currents over at the two different altitudes sampled by these payloads. For the expected variations over the relatively short time a distance scales separating the features traversed by the two payloads as achieved with original TRICE mission, we will be able to directly measure how field aligned current varies along field-lines in the cusp ionosphere.

Another key feature of the cusp is its role as a source of ion outflow for the magnetosphere. The SCIFER results suggested that field-aligned currents are associated with ion heating. *Strangeway et al.* [2000] found that there was a correlation between Poynting flux into the ionosphere and ion outflows and suggested that some of this Poynting flux is dissipated into heating ions and their subsequent outflow. However the correlation is not one-to-one between local Poynting flux and local ion outflow. The correlation is strongest between peak Poynting flux and peak ion outflow over the entire region of electromagnetic energy input and ion heating. The *Strangeway et al.* [2000] study was performed using FAST data which were somewhat compromised by not having a full vector electric field in the plane perpendicular to the background magnetic field. This led to some ambiguous cases in which it appeared that the Poynting flux was directed away from the ionosphere. The TRICE-2 payloads will have a full vector $E_\perp$ measurement and this will allow unambiguous determination of the direction of the Poynting flux. In addition, it is likely that the TRICE-2 high-flyer will penetrate regions of ion heating. By making direct measurement of Poynting flux which is associated with ion heating events, TRICE-2 will address the question of whether the Poynting flux and heating correlate locally, resolving the ambiguities in the *Strangeway et al.* [2000] results.

Analysis of optical emissions in poleward moving auroral forms, a standard feature of the cusp for B_Z southward, shows that these are composed of electrons of keV and greater energies, implying an electron acceleration mechanism below the reconnection site. It is an open question which mechanisms contribute to this acceleration. For example, if Alfvén waves accelerate the electrons as under some conditions in nighttime aurora, the rockets will be instrumented to detect the waves and particles signatures of that interaction. If significant parallel electric fields exist below the height of the upper rocket (≥ 1200 km), comparing electric field mapping between the rockets may reveal this.

Chaston et al. [2007] developed a large database of FAST cusp crossings showing 100% occurrence rate of Alfvėn waves in the cusp, and estimating that 50% of the electron acceleration observed there results from Alfvén wave-electron interaction. A number of experiments, including SCIFER [e.g., *Kintner et al.,* 1996] and FAST [e.g., *Chaston, et al.,* 2006] , demonstrated a correlation between transverse accelerated ions (TIA), reduced electron density, broadband low frequency electric field fluctuations, and electron precipitation. *Chaston et al.* [2006] describe a mechanism linking these observations, starting with a flux of shear Alfvén waves generated in the magnetosphere and impinging on the ionosphere from above. These invariably encounter some irregularity or non-laminar feature in the topside ionosphere and are somewhat focussed, leading through refraction to a finite perpendicular wavelength and a change in the nature of the Alfvén waves which become dispersive, with a parallel electric field that accelerates electrons. The electrons in turn drive waves such as lower hybrid waves. TIA can result from a variety of processes, driven by the waves generated by the electrons or by the dispersive Alfvén waves directly. In the diverging field geometry the accelerated ions escape, and the resulting loss of plasma reinforces the density cavity that focussed the Alfvén waves to begin with. The positive feedback leads to development of large scale density depletion in the cusp ionosphere and significant ion outflow "cusp ion fountain." Several significant details of this mechanism have been observed, such as FAST measurements expected perpendicular phase velocity and Poynting flux associated with the focussed Alfvén waves [*Chaston et al.,* 2006]. Experiments and associated modelling have proven the existence of Alfvénic electron acceleration in the cusp [e.g., *Tanaka et al.,* 2005; *Su et al.,* 2004]. Various physical mechanisms leading to cusp ion outflow are described by *Strangeway et al.* [2005].

However, there remain significant questions about Alfvén waves in the cusp. For example, the extent of the region which a given wave field covers is not known because reported measurements have been from single spacecraft. If Alfvén waves observed in the cusp are the signature of time-varying reconnection due to an extended X-line, as one would expect from the time varying field associated with this process, then the longitudinal extent should be relatively broad and both TRICE-2 payloads should see similar signatures, even when separated by tens of km. Because the transverse separation varies over a wide range for the TRICE-2 mission we will be able to test a range of perpendicular scales over which similar Alfvénic activity is observed. Should we be fortunate enough to observe a clear signature of the same wave on both payloads during the period when they are nearly conjugate, then we can further study the detailed character of the wave by doing timing analysis. This allows a determination of the perpendicular wave number and would confirm the determinations of scales sizes of the order of the plasma skin depth [*Chaston et al.*, 1999; *Chaston et al.*, 2003; *Andersson et al.*, 2002].

The cusp is a rich source of plasma waves at all altitudes, many of the generated by the non-thermal electron and ion distributions described above, as measured by many spacecraft including Viking [*Pottelette et al.,* 1990], FAST [*Pfaff et al.,* 1998], and sounding rockets such as SCIFER and TRICE-1. Measurements of these waves are an important component of TRICE-2 because they provide signatures of open/closed field line boundaries, they provide an independent measurement of plasma density and other parameters, and they reveal important mechanisms whereby energy is redistributed to particles. These waves include broadband low frequency waves associated with electron precipitation and involved in transverse ion acceleration, as described above. They also include Langmuir and Langmuir-whistler modes excited by the accelerated electrons, which can attain significant amplitudes (hundreds of mV/m). It has been speculated that similar waves may play a significant role in determining the background electron temperature in the nighttime aurora [e.g., *Beghin et al.,* 1989; *Kintner et al.,* 1995].

Cusp Langmuir waves occur in short-duration bursts and are strongly modulated at frequencies ranging from < 1 kHz to > 50 kHz [e.g., *Bonnell et al.,* 1997; *Stasiewicz et al.,* 1996; *LaBelle et al.,* 2010]. The strong modulation presumably results from mixing of parallel and oblique Langmuir

wave modes, but the detailed wave physics is controversial. The standard picture, suggested by Freja observations of *Stasiewicz et al.* [1996], involves generation of oblique modes via nonlinear wave-wave interactions involving lower hybrid or other low frequency modes. *LaBelle et al.* [2010] based on TRICE-1 data suggest instead that the different wave modes may be excited by linear processes and that the mixing occurs due to inhomogeneity in the plasma. Recently *Sauer and Sydora* [2011, 2012] observed in simulations evolution of much longer wavelength Langmuir waves in the beam-plasma interaction with $f_{pe} < f_{ce}$, suggesting a third possibility for the strong modulation observed in cusp Langmuir waves. Despite their occurrence in a wide range of space and laboratory plasmas as a direct consequence of beam-plasma interaction, Langmuir waves present some fundamental physics problems, and the cusp, where the strong modulation is consistently observed, is a good laboratory to investigate these.

Our proposed pair of suitably instrumented rockets passing through the ionospheric cusp during steady IMF B_Z southward conditions with a variety of spatial and temporal separations will provide a wealth of new information on cusp ionosphere. These data will be used to answer outstanding questions about the character of magnetopause reconnection and cusp electrodynamics.

3 Relevance to NASA Science

The TRICE-2 proposal is highly relevant to NASA's 2014 Strategic Plan. It directly relates to Objective 1.4: *Understand the Sun and its interactions with Earth and the solar system, including space weather.* Reconnection is a fundamental process in the interaction of the Sun with the Earth, and, currently, it is not known if this process is inherently unstable. Explosive reconnection is known to occur in solar flares and in the magnetotail, but there is evidence that the process may occur quasi-steadily at the magnetopause. However, reconnection may occur quasi-steadily on long time-scales and still have large variations in the reconnection rate at much shorter timescales. That reconnection is a central science focus for NASA is clearly demonstrated by the upcoming launch of the MMS mission in 2015. The MMS mission focuses on the detailed physics of a single, localized reconnection region while TRICE-2 provided a more synoptic, large-scale picture of the reconnection process. TRICE-2 provides a complimentary approach to understanding reconnection and will definitively determine whether reconnection is inherently unstable at a wide range of timescales from minutes to seconds.

TRICE-2 also directly relates to the science goals of Helophysics section of NASA's 2014 Science Plans, specifically, *Advance our understanding of the connections that link the Sun, the Earth, planetary space environments, and the outer reaches of our solar system.* The cusp is one location where there is strong coupling between the magnetopause/magnetosphere and ionosphere/upper atmosphere. The dual-altitude measurements from TRICE-2 will elucidate electrodynamic processes such as field-aligned currents and ion heating that have both local and global consequences on magnetosphere/ionosphere coupling.

It is also worth noting that the recent NRC decadal survey for Heliophysics strongly supports the use of the sounding rocket program as an important element of the Helipphysics science mix. TRICE-2 provides an excellent opportunity for science and student training of exactly the type lauded by the NRC.

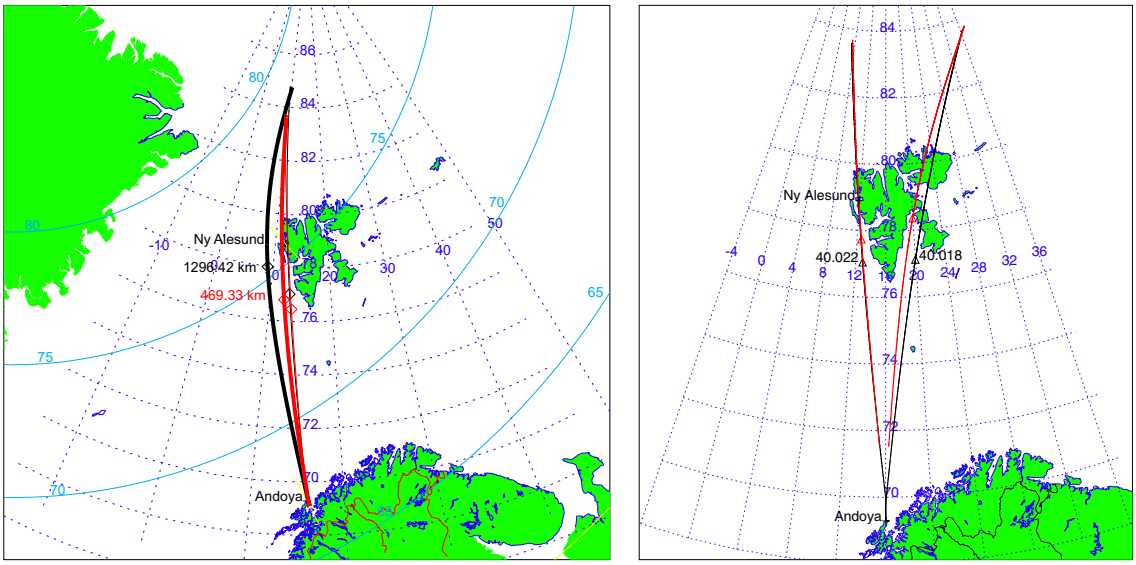

Figure 3: Model trajectories for a Black Brant X (thin red line) and Black Brant XII (thin blue line) launched from Andoya Rocket Range on the left hand side. The thick lines show the trajectories as mapped along magnetic field lines to a constant altitude of 110 km. The right hand side shows the actual trajectories achieved for the original TRICE mission.

4 Proposed Twin Rocket Investigation of Cusp Electrodynamics 2: Operational Aspects

For the TRICE-2 mission, we propose to launch two payloads along nearly the same set of geodetic coordinates but at differing times and to different altitudes. The resulting time difference in when the payloads cross a given magnetic latitude allows us to compare the predicted evolution of the stepped ion dispersion signatures which are associated with magnetopause reconnection to determine whether this is a temporal or spatial phenomenon (or both.) The difference in altitude will cause the separation between the payloads in the north-south direction to vary as a function of time because the low-flyer overtakes the high-flyer due to its lower apogee. This variable baseline in the north-south direction will allow us to determine which features are transitory and which are stable in time because as the separation in time and space becomes smaller, temporal variations will diminish, but spatial variation will remain. In addition, the two altitudes yield a set of measurements which allow us to better understand the electrodynamics of the cusp region and the relationship between in situ measurements and ground-based observations. The payloads will include DC and high frequency electric field measurements; high time, energy, and pitch angle resolution electron and ion distribution measurements; and electron density measurements.

We propose that the two payloads be launched from the Andoya Rocket Range in Norway. Our requirements are that one payload will fly to altitude of 1100 km or greater and the second payload will fly to an altitude of $\geq$ 450 km. The original TRICE mission was planned as a high-flyer payload launched on a Black Brant XII and a low-flyer would be launched on a Black Brant X. Figure 3 shows the original model trajectories for this configuration on the left hand side. On the right hand side of Figure 3 we show the actual trajectories for the original TRICE mission which were achieved with a pair of Black Brant XII vehicles. As can be seen, the plan had two rockets flying in essentially the same direction and have very similar impact points. The low-flyer reaches an apogee of somewhat less than 500 km

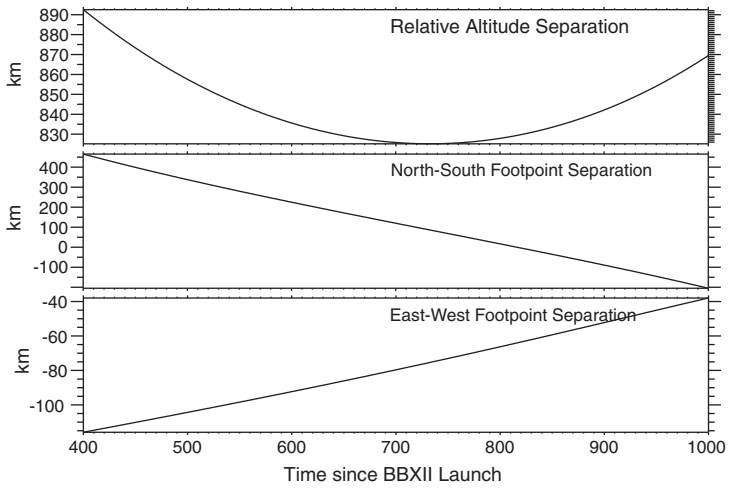

Figure 4: Altitude, east-west, and north-south separations of the ionospheric footpoints of the high-flyer and low-flyer payloads as planned for the original TRICE mission. The actual longitudinal separation achieved reached a maximum of 150 km.

whereas the high-flyer reaches an apogee of almost 1300 km. This means that the flight time for the low-flyer is significantly shorter than that of high-flyer by approximately 500 s. As flown, the high-flier deviated from the planned trajectory due to vehicle performance issues with one of the motors which have since been rectified with the latest equivalent rockets. Even with this deviation, which is close to worst case, the trajectories are still sufficiently close that both rockets traversed the cusp region and the PMAF structures within the cusp. *Fuselier et al.* [2002b] showed that cusp aurora for southward IMF (our planned IMF condition) have a local time extent of 4 hours which is of the order of 1000 km, and quite large compared to the 150 km maximum separation of the original TRICE rockets. Additionally, *Fasel et al.* [1995], showed that dayside poleward moving auroral forms (one of the features we use in our TRICE-2 launch criteria) have latitudinal extent of 50-100 km and longitudinal extent of 500-1000 km consistent with the *Fuselier et al.* [2002b] result. That is a factor of 3-8 times larger than the 150 km maximum longitudinal separation of the original TRICE rockets, demonstrating high probability of achieving the trajectories needed for the proposed science.

Operationally, the scenario for the original TRICE mission launched the low-flyer 2 minutes after the launch of the high-flier. We would plan to repeat this timing. This has three advantages: 1) operationally it is difficult for the range to deal with launches that are any closer together in time; tracking and TM are significantly complicated by rockets which are too close together; 2) the agogees of the payload are then aligned in time so as to produce the best conjunction between the high and low payloads when they are at the smallest field line separation; and 3) this provides a variable separation which is valuable for confirming conclusions about spatial versus temporal effects. This is illustrated in Figure 4 which shows originally planned altitude, magnetic north-south, and magnetic east-west separations as a function of time since launch of the high-flyer payload for a scenario in which the low-flyer is launched 4.5 minutes after the high-flyer. The actual separations were similar, but the longitudinal separation reached 150 km, rather than the planned 40 km. As can be seen, the initial north-south separation is quite large, but the low-flyer overtakes the high-flyer and then runs ahead. In time this means that the low-flyer initially samples the cusp region some 4 minutes after the high-flyer, but eventually catches up and is sampling the cusp approximately 2 minutes in advance of the high-flyer. This provides us with both temporal and spatial separation to allow comparison of the stepped ion dispersion features to determine if they move

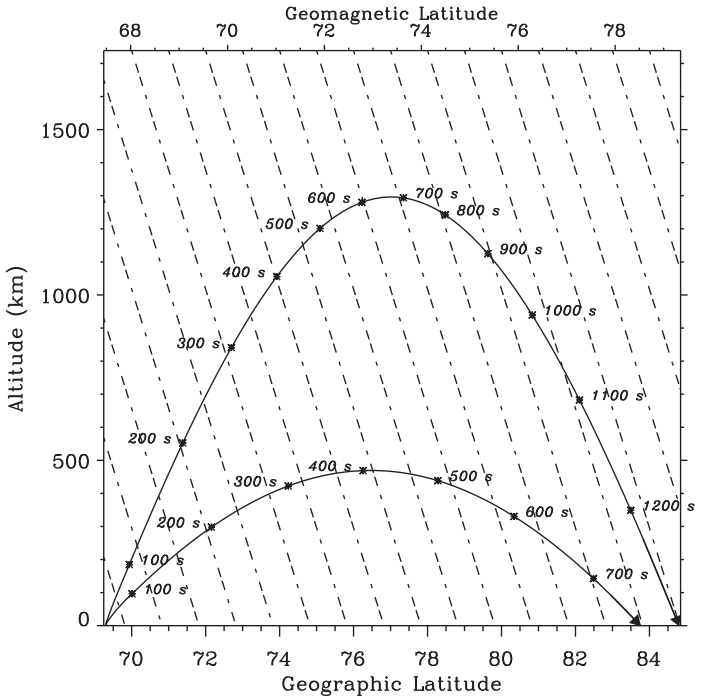

Figure 5: Range vs. altitude of the two payloads as function of time since launch of each payload. The Earth's magnetic field lines have been added to illustrate how the two payloads map from one altitude to the other.

with time or if they are spatially fixed.

To illustrate the mapping between the payloads, Figure 5 shows how the two payloads cross field lines as a function of time since launch. As can be seen, an offset in launch time of 2-5 minutes produces the best conjunctions near apogee of the two payloads. Once exact payload weights are determined, so that trajectories can be accurately predicted, we will optimize the difference in launch times and azimuths to produce the best range of temporal and spatial separations for both investigation of cusp ion signatures as well as electrodynamic features.

The launch criterion will be based on a combination of upstream solar wind monitoring provided by the ACE spacecraft (presumed to still be operational in the Winter of 2018/2019) combined with optical observations from Svalbard and radar observations from SuperDARN and EISCAT. The desired solar wind conditions are to achieve steady solar wind velocity and density during a period of continuous southward IMF B_Z. However, because IMF B_Y has a significant effect on the cusp location and current system orientation, we desire conditions in which IMF clock angle is predominantly in the southward direction, that is, conditions under which IMF $|B_Y| < |B_Z|$. Optical instrumentation on Svalbard include all-sky cameras, and multi-channel meridian scanning photometers which will be used to determine the presence of poleward moving auroral forms along the projected rocket tracks. The poleward moving auroral forms have been found to be associated with the ion steps that we wish to measure [*Lockwood et al.*, 2001]. By launching only when the rocket trajectories will traverse these forms, we can further test this association and have high probability of crossing the ion dispersion signatures that we desire. The radar measurements will provide the overall electrodynamics configuration and will allow us to determine that the rockets will traverse a region of anti-sunward convection.

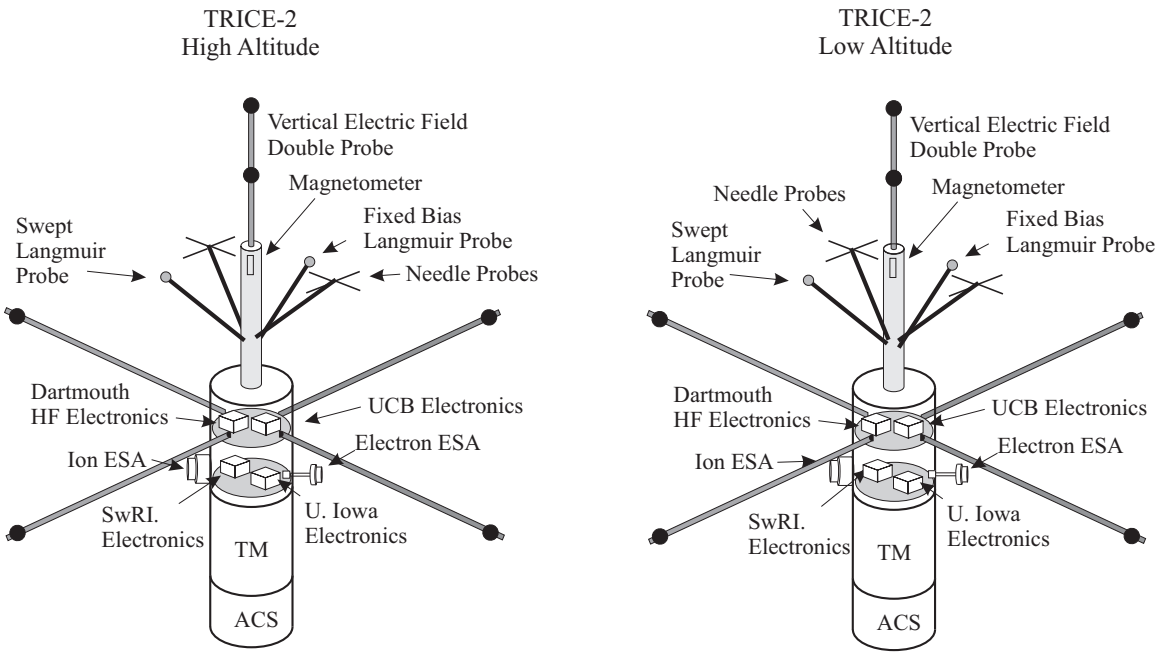

Figure 6: Layout of the TRICE-2 payloads. All booms are shown in their deployed positions.

5 Proposed Twin Rocket Investigation of Cusp Electrodynamics 2: Instrumentation

Figure 6 shows sketches of the proposed TRICE-2 payloads. They include electric field booms and electronics, particle detectors with associated booms and electronics, and a magnetometer. HF electric field probes, the science magnetometer, and Langmuir probes are mounted on a short axial boom forward of the payload. A total of four telemetry links will be needed, two for each payload. Each payload will have one 5 MHz baseband link and one PCM link running at 6-10 Mbits/s (depending on the exact amount of telemetry needed). The successful acquisition of all telemetry links for the original TRICE mission demonstrates that although achieving this set of links is not trivial, it is clearly feasible. Attitude control and knowledge is required for both payloads, Post-flight determination of the attitude to within 5° is required. As mentioned above, the desired apogee for the high-flyer is $\geq$ 1200 km, and for the low-flyer, 400-500 km. The launch azimuth will be somewhat east of magnetic north to put the payload apogees over Svalbard to allow the best conjunction with ground-based instrumentation. A two week window of 3-6 hours per morning centered near local noon and during Moon-down conditions will provide multiple launch opportunities.

5.1 Electric and Magnetic Field Measurements

The double probe technique will be used for both the DC electric field and wave measurements. The UCB Fields package provides measurement of the DC and low-frequency electric and magnetic fields, as well as the electric component of ELF/VLF waves up to 20 kHz, as well as providing the sensor surfaces for HF wave measurements up to 5 MHz by the Dartmouth College fields package.

The E-field boom system consists of four (4) rigid metallic (BeCu) stacer booms deployed in a cruciform array in the plane perpendicular to the long axis of the science payload from deploy units

mounted near the front of the science payload. The E-field boom deploy unit will be a quad-boom unit, with all four of the stacer booms held and released by a single actuator and gear train which provides for a slow (20-s) and symmetrical deploy of the entire array, minimizing tip off and other unwanted dynamical perturbations. Note that the quad-stacer unit is designed to be a deck of the payload section, rather than mount to a separate deck in order to reduce mass.

Each boom is 3 meters long (stroke) resulting in a tip-to-tip double probe length of 6.5 m. Each boom will include two electrically-isolated surfaces: The first, consists of a spherical graphite-coated hollow aluminum spherical electrode at the tip of the boom (8-cm nominal radius) used for the E-field measurement. The second, consists of the exposed portion of one of the stacer booms themselves that will be used as capacitively-coupled sensor surfaces for the HF measurement in conjunction with the Dartmouth College fields package. The use of an exposed portion of the stacer for the high frequency measurements provides a convenient method for providing sensor separation and does not affect the DC and lower frequency measurements as past experience has shown. The stacer boom surface will be covered with a coating to meet mechanical and electrical specifications for charging and lubrication.

In addition to the stacer booms, a fixed boom projecting forward from the top deck parallel to the spin axis will hold the science magnetometer provided by UCB; two small spherical probes for measuring the HF parallel electric field; a pair of spherical Langmuir probes, one a fixed-bias measurement and the other a swept Langmuir probe measurement; and two small booms each with 4 needle Langmuir probes. This design has been utilized successfully on several past missions. The Langmuir probes will provide information about the density and temperature of the background electrons. Dartmouth/UI provided a similar configuration of electric field booms, probes, and preamplifiers for the successful recent ACES and CHARM-2 rockets. For magnetic field measurements, we will use a purchased, commercial three-axis fluxgate magnetometer, nominally the Billingsley TFM100.

The Fields electronics consists of harnessing and preamplifiers for the E-field sensors, harnessing for the B-field sensor, and the Fields Electronics Box (FEB). The E-field preamplifiers are body-mounted in the FEB with a coax line running up the center of the stacer boom to the E-field sensors at the tips of the booms as well as through the FEB-to Stacer harness. The shield of the coax is electrically isolated from the stacer and harness, and is driven with a suitably filtered version of the preamp output so as to mitigate the impact of cable capacitance on sensor input impedance (input guarding or bootstrapping). Design of the E-field and density preamp units follows the designs used in the THEMIS-EFI, RBSP-EFW, and GREECE (Samara 36.287) units for the E-field functions (Bonnell et al., 2008). The E-field preamps run off a fixed +/- 15-V analog supply, rather than the floating supplies used in the deep space models. This is allowed as floating potentials during nominal ionospheric and auroral operations are a few volts, rather than the tens of volts found in low-density magnetospheric environments.

The FEB will be mounted to a science payload deck, with appropriate front-panel connectors for all signal, power, and command lines. The FEB comprises 3 electronics boards that implement the Power Supply, Analog Signal Conditioning, and Digital Signal Processing. The Power Supply Board (PSB) generates the necessary regulated internal power services from unregulated payload power input; provide housekeeping data for power supply functions; and generates analog power- and actuator-related housekeeping data (current, voltage, and temperature monitors; deploy state monitors; etc.). The Analog Processing Board (APB) shall provide analog signal conditioning for all fields sensor inputs (E, B). The Digital Electronics Board (DEB) provides sampling and analog-to-digital conversion for all fields sensor inputs; provide sampling and analog-to-digital conversion for all fields housekeeping data; and provide serial data interface for all data (housekeeping and science) from Fields package to Payload TM module.

Design of the APB and DEB is analogous to boards in the THEMIS and RBSP-EFW Instrument Data Processing Units (IDPU) and GREECE Fields Package (Boom Electronics Board, BEB; Digital

Fields Board, DFB; [*Bonnell et al.*, 2008; *Cully et al.*, 2008]. Design of the PSB will follow that of the analogous boards in the THEMIS and RBSP-EFW IDPUs and the GREECE Fields package [*Taylor et al.*, 2008], with the exception that commercial off-the-shelf switching power supply modules will be utilized rather than the custom switching supplies used for satellite missions. Efforts to keep switching supply frequencies above the top of the nominal DC-VLF science band ($\geq$ 20 kHz) will be made. EMI filters on all experiment power supplies will also effectively reduce such interference to an adequate level as on many previous flights involving VLF and HF receivers.

The Fields package will produce two channels supporting a continuous two-axis estimate of the component of E in the plane perpendicular to the long axis of the payload (nominally, perpendicular to B) at 312.5 samp/s (156.25 Hz Nyquist) with a +/- 1 V/m dynamic range at 16-bit resolution; three channels supporting a continuous three-axis measurement of the B-field at 312.5 samp/s (156.25 Hz Nyquist) with a +/- 50,000 nT dynamic range at 16-bit resolution; four channels supporting sensor potential and interferometric measurements (sensor to skin) at 325 samp/s (156.25 Hz Nyquist) with +/- 13 V (4.6 V/m) dynamic range at 16-bit resolution; three (or six) channels supporting a one- (two)-axis estimate of E from 10 Hz to 20 kHz along with two-sensor interferometric measurements (sensor-to-skin) at 40-ksamp/s (20-kHz Nyquist) with a +/- 200 mV/m dynamic range at 16-bit resolution.

Dartmouth College will provide high-frequency (HF) wave receivers to each payload. The sensors will consist of spherical probes separated by 30 cm along a fixed fiberglass boom of at least 60 cm length projecting forward from the top deck of the rockets. The relatively short probe separation, parallel to the rocket axis and hence approximately parallel to the magnetic field, is ideal for measuring cusp Langmuir waves which have predominantly parallel electric fields. Preamplifiers operating over the frequency range DC-5 MHz will be integrated into each probe. The resulting signals will be analyzed by the Dartmouth HF receiver, which covers 100 kHz-5 MHz, and by several channels in the UCB ELF/VLF receiver, described above, which operates at lower frequencies. The HF receiver uses a dedicated analog telemetry channel, using band limiting and automatic gain control to ensure optimal performance despite relatively low dynamic range on the TM link. This experiment has signficant flight heritage including Auroral Turbulence-2 and PHAZE-2 (1997), RACE and SIERRA (2002), HIBAR (2003), TRICE-1 (2007), and CHARM-2 (2010). In all these cases, the instrument not only detected a host of natural wave modes such as whistler, Langmuir, and upper hybrid, together with associated fine structure, but it also detected multiple wave cutoffs over large portions of the flights, providing reliable high time-resolution absolute electron density measurements. This last capability is a major contribution to TRICE-2.

In addition, on the high-flyer payload only, Dartmouth will provide preamplifier electronics to detect high-frequency voltage fluctuations induced in one of the UCB Weitzmann boom elements. This element, more than two meters long and perpendicular to the rocket axis, comprises a monopole antenna that, while not ideal for detecting weak Langmuir waves, is easily able to respond to large amplitude ones approaching 100 mV/m. The signal from this effective monopole antenna will be processed with the same type of HF receiver described above. Both HF receivers will be calibrated for group delay, so that timing between the signals, corresponding to sensor pairs separated by approximately one meter parallel to the magnetic field, can be used to estimate the phase velocity along the antenna separation line, parallel to the magnetic field, and hence the parallel wavelength of the Langmuir waves. The phase comparison will be achieved by digital downconversion: both signals will be digitized at a relatively low rate, 50-100 ksamples/second, and multiplexed onto the main PCM telemetry transmission. Because Langmuir waves dominate the 100 kHz-5 MHz instrument passband when they occur, they will be effectively aliassed into the much narrower band defined by the Nyquist frequency (half the sample rate). Because the Langmuir frequency will be known from the waveform measured on the forward axial boom pair (transmitted fully to ground on the high-bandwidth analog TM link), the phase between the

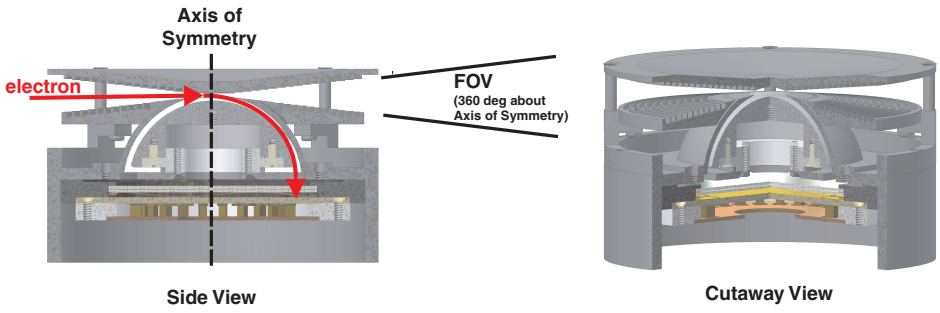

Figure 7: Side and cutaway views of the 'top-hat' electrostatic analyzer.

original high-frequency Langmuir wave signals can be inferred from the phase between the aliassed signals in the sampled waveforms. The technique has limitations, in that it fails if the aliassed waveforms happen to fall on zero frequency or on the Nyquist frequency, but to achieve the science goal it is not necessary to measure the wavelength of every Langmuir wave encountered on the flight; a small selection will suffice to test whether the parallel wavelengths of Langmuir wave components are consistent with the resonance condition with low-energy cusp electrons, or is much longer as suggested by *Sauer and Sydora* [2011, 2012]. The variation of density as the rocket ascends in the inhomogeneous ionosphere will assure that not all, but only a small percentage, of the encountered plasma frequencies will alias to zero frequency or the Nyquist frequency. For most of them it will be possible to measure their wavelengths with sufficient accuracy to test predictions of *Sauer and Sydora* [2011, 2012] using this method. The method has been extensively explored numerically and found effective, and it has been demonstrated in previous flights that the Dartmouth HF wave receivers detect coherently enough to measure small phase differences of $>$ 1-MHz signals. For example, on the recent CHARM-2 flight, the left-hand polarization of auroral roar emissions was confirmed very accurately by the Dartmouth receivers (virtually no false detection of right-hand component as expected from even small phase detection errors) [M. Dombrowski, personal communication, 2014]. This scheme exploiting digital aliassing to measure phase differences between high-frequency signals is a novel technique but represents minimal risk to the TRICE-2 experiment since its function is not critical to the main mission science.

5.2 Electron Measurements

The University of Iowa will provide each TRICE-2 payload with an ElectroStatic Analyzer (ESA) to measure electron distributions. These electron ESA's provide high time resolution measurements while retaining very good energy coverage. This is crucial for accurate determination of the variation in electron distributions in the cusp region which can vary over short scales. The basic design of the ESA analyzer that we propose is sketched in Figure 7 and is identical to ones that have been designed and successfully flown by the PI of this proposal for several rocket flights including Thunderstorm III, Auroral Turbulence I and II, RACE, HiBAR, ACES, and CHARM-2 missions. Based on an original design by C. W. Carlson and G. Paschmann, this ESA is an imaging type device that counts single ions or electrons having a desired energy with a velocity vector lying within an azimuth plane. The ESA is cylindrically symmetric, and this diagram is a section along the axis of the detector. The dashed line in the figure is a representative trajectory of a particle which is counted and shows how particles which enter the detector in the aperture plane (upper left in the figure) "see" the attracting potential on the inner hemisphere through the hole in the outer hemisphere and are pulled out of the aperture plane into the gap between the hemispheres. Particles entering with a specific azimuth in the aperture plane are

imaged onto a corresponding azimuth in the sensor plane. If the magnetic field lies near to the aperture plane, then all pitch angles may be sampled simultaneously. Microchannel plates are used as sensors, followed by typical charged-sensitive amplifiers.

On the original TRICE mission flown in 2007, all of the UI particle detectors failed due to arcing in the high voltage supples. A subsequent investigation of the cause determined that a change in type of high-impedance feedback resistor used in the supplies led to the failures. The part used in TRICE appeared to be solid, but, in fact, had a hollow core. Under flight conditions, in which the pressure drops to vacuum in 1-2 minutes, this hollow core traps air which slowly decreases in pressure until the resistor interior reaches the corona pressure. At this pressure, the several megohm resistor becomes a rather good conductor and delivered full voltage to the feedback op-amp thereby destroying the HV supply. It also turns out that other rocket experimenters had experienced the same problem. Since that time, we verify and use only solid core resistors and have had two successful flights (ACES, CHARM-2) with no HV supply issues, even though on ACES, HV supplies were turned on at 100 km.

These particle measurements will be used for determining electron spectral characteristics in regions where poleward moving auroral forms are observed, as well as for identifying the boundary between closed and open field lines by observing the boundary of higher-energy trapped electrons. We propose to step each of the electron detectors through 36 energy steps over the range 20 eV to 10 keV in 48 ms. Consequently, we will obtain a complete distribution function every 48 ms. Using a typical ground track velocity for a rocket of $\sim$ 1 km/s, this gives us a spatial resolution of the electrons of the order of 50 m. Given the geometric factor of the detectors and typical fluxes in the auroral region, accumulation intervals of 1 ms will produce good count levels and allow rapid determination of the particle spectrum. The electron ESA detector measures a full range of pitch angles simultaneously because the variation of the distribution as a function of pitch angle can offer substantial information about the electron-wave interactions. For the electrons, we will use 10° bins to cover the full 180° of pitch angle.

5.3 Ion Measurements

Southwest Research Institute (SwRI) will provide each TRICE-2 payload with a large geometric factor ion detector to provide high time resolution of ion distributions without mass identification. The ion measurements are important for identification of the dispersed ion signatures of dayside reconnection as well as for detection of small-scale regions of transverse ion acceleration. These detectors utilize the same instrument geometry as the electron ESA detector discussed above, but the toroidal tophat ESAs are made larger to compensate for the lower differential energy flux presented by ions so that a good count rate is achieved.

The rocket's magnetic ACS will align the spin axis with the ambient magnetic field direction so that the ions which leave the exit aperture are mapped in an image plane which maps to pitch angle. Each image plane consists of 20 pixels of various sizes, with the largest subtending 11.25° of pitch angle and the smallest 3.75°. The smaller pixels are used to cover the pitch angle range near 90° in order to sample the transversely-accelerated ions with good resolution. In order to achieve high time resolution, the instruments will be swept from 10 eV to 15 keV in 50 exponentially-spaced steps (ΔE/E=10%), with each step lasting 1 ms, so distributions will be measured at a rate of 20/s. The geometric factors of these instruments (a total of 0.01 cm^2-s-sr keV/keV) are large enough to make statistically-significant measurements at this rate for the flux levels expected to be encountered. The sensors are deployed on short booms (30 cm) during flight to minimize interference from the rest of the payload. These instruments and their electronics are nearly identical to electron and ion instruments developed by SwRI for the Rosetta-IES, Juno-JADE, RBSP-HOPE, MMS-DIS, MMS-HPCA, the GREECE rocket.

5.4 Langmuir Probe

The University of Iowa will also provide swept and fixed bias Langmuir probes. The Langmuir probes provide absolute and relative electron density measurements to confirm the density inferred from wave cutoffs using the 0-5 MHz high frequency receiver [*McAdams et al.*, 1998]. The swept probe runs at lower rate and provides data to normalize the relative density profile obtained from the fixed-bias probe which is run at higher sampling rate. The designs will be copies of the the fixed and swept probes that UI has successfully flown on multiple rockets. UI has extensive experience in analysis of swept Langmuir probe data to determine background electron temperature and density [*Kletzing et al.*, 1998]. The result will be a reasonably reliable electron density profile from the whole flight, upleg and down, which will constrain electron density models used in ray-tracing observed ray signatures, for inferring source locations and sizes, etc.

5.5 Langmuir Needle Probes

To provide ambient electron density measurements which are independent of the wave measurements, TRICE-2 will include the University of Oslo (UO) Langmuir probe system for high resolution measurements of space plasma density. The system consists of four or more cylindrical needle probes, and the four needle system is referred to as the 4-Needle Langmuir Probe system (4-NLP). Each probe is positively biased, with a different bias for each probe. The probes typically have a diameter of 0.5 mm and a length of 25 mm. In the ionosphere the Debye length (plasma charge shielding distance) is typically 1 cm, i.e. much larger than the probe diameter and plasma shielding effects can be neglected. In this environment the collected electron current Ie will be in the range from 1 nA - 1 μA for positive probe potential V_p of a few volts relative to the plasma [*Bekkeng et al.*, 2010]. A crucial feature of the m-NLP technique is that dI_e^2/dV_p is a function of electron density squared (n_e^2), independent of the electron temperature T_e and the spacecraft potential [*Jacobsen et al.*, 2010]. It can cover the electron density range from 108-1013 m^{-3}. The probes have been tested in the plasma chamber at ESTEC and proved to work perfectly for sampling rates up to 10 kHz. The 4-NLP system was successfully flown on the ICI-2&3 rockets launched from Svalbard into the cusp ionosphere in 2008 and 2011, providing absolute electron density measurements to meter scales [*Moen et al.*, 2012]. This instrument also has flight heritage on three ECOMA flights from Andya (mesospheric plasma dust mission) in 2010, and an 8-NLP system was flown on the NASA MICA flight from Alaska (F-region/night time auroras) in 2012.

5.6 Ground Measurements

The University of Oslo will provide ground measurements from sites on Svalbard. These measurements will include multi-channel meridian scanning photometers and all-sky cameras from Ny-Ålesund and Longyearbyen. These two stations are at the same magnetic longitude, but a different magnetic latitudes and very nearly conjugate to the TRICE-2 apogees. The optical measurements, which are available in realtime, will be used to determine the characteristics of poleward moving auroral forms and will be important for both the launch decision as well as for post-flight data analysis. In addition, The Oslo group will work with us to acquire EISCAT observing time in support of the rocket launches.

The University of Leiceister will provide ground-based measurements in the form of SuperDARN radar network support and will also work with us to put together and multi-associate bid (along with the Oslo group) for EISCAT time in support of the TRICE-2 mission. These measurements will be available in realtime over the web and will be used for the launch decision as well for scientific data analysis. These radar measurements will be important for providing the large-scale ionospheric context for the interpretation of the TRICE-2 in situ data.

6 Proposed Twin Rocket Investigation of Cusp Electrodynamics 2 Work Plan

The principal investigator for TRICE-2 is C. Kletzing who will oversee all work at University of Iowa, including design and construction of the electron detectors, associated electronics, and design and construction of the frequency Langmuir probes. The P.I. will be responsible for all documents and meetings required by NASA as well as for overseeing publication of scientific results from the mission. Design and construction at UI will be carried out by research scientist Scott Bounds along with a graduate student. Dr. Bounds will also serve as payload manager and liaison among the various groups involved in TRICE-2. Data analysis done by the student will form the basis of the student's dissertation. All personnel, including the PI, will support design reviews and integration and testing of the payload.

Co-Investigator J. LaBelle will oversee all work at Dartmouth College including design and construction of preamplifiers and four high frequency receivers. Design and construction at Dartmouth will be performed by engineer D. McGaw together with a graduate student. As in previous experiments, the instrument development, data analysis, and related theory will form the major portion of the graduate student's PhD dissertation. These Dartmouth personnel will also support integration of the payload.

Co-investigator J. Bonnell will oversee all work at UCB including construction of electric field booms and probes, design and construction of low frequency electric field electronics. UCB will also provide the science magnetometer along with associated high resolution sampling electronics. A graduate student will assist Dr. Bonnell in design and construction of the UCB instrument package, and data analysis done by that student will form the basis of that student's Ph.D. dissertation.

Co-investigator S. Fuselier will oversee all work at SwRI including design and construction of large-geometric factor ion detectors for both payloads.

Co-investigator J. Moen will oversee all work at Oslo University including design and construction of the Langmuir needle probes for both payloads.

Co-Inverstigator K. Trattner will oversee all work at the University of Colorado/LASP and will provide scientific support for mission planning as well as analysis of flight data.

We anticipate conducting the Mission Initiation Conference for this flight in third quarter 2015, with a design review $\sim$12 months later. Hardware will be delivered to Wallops Island for integration in the second half of 2018, at a schedule to be determined by Wallops Flight Facility. The two week launch window is best scheduled for November/December, 2018 during Moon-down conditions at the optical observing sites on Svalbard. Following the launch, data will be analyzed and scientific results will be presented at AGU or other international conferences starting in the second half of 2019.

7 Conclusion

We propose a pair of rockets, launched approximately four minutes apart and with different apogees to probe the cusp. The primary science goals are to measure the ionospheric signatures of dayside reconnection and to investigate the electrodynamics of the cusp region. By having different launch times and apogees, but similar launch directions the two rockets will traverse the cusp with a set of east-west and north-south separations that ranges from nearly conjugate to of the order of 100 km due to the differences in altitude. The payloads will also traverse a given magnetic latitude at different times. Taken together, this set of temporal and spatial separations will give us a unique data set that will produce tests of a variety of physics including steady versus pulsed reconnection, current closure, and particle energization. The TRICE-2 mission promises to reveal an exciting array of new data to expand our knowledge of the cusp region.

References

Andersson, L., N. Ivchenko J. Clemmons, A. A. Namgaladze, B. Gustavsson, J.-E. Wahlund, L. Elliason, and R. Yu. Yurik, Electron signatures and Alfvén waves, *J. Geophys. Res.*, *107*, 2002.

Beghin, C., J. L Rauch, and J. M. Bosqued, Electrostatic plasma waves and HF auroral hiss generated at low altitude, *J. Geophys. Res.*, *94*, 1359, 1989.

Bekkeng, T. A., K. S. Jacobsen, J. K. Bekkeng, A. Pedersen, T. Lindem, J-P. Lebreton, and J. I.Moen, Design of multi-needle langmuir probe system, *Meas. Sci. Technol.*, *21*, 085902, 2010.

Bonnell, J., P. Kintner, J.-E. Wahlund, and J. A. Holtet, Modulated Langmuir waves: observation from Freja and SCIFER, *J. Geophys. Res.*, *102*, 17233, 1997.

Bonnell, J. W., F. S. Mozer, G. T. Delory, A. J. Hull, R. E. Ergun RE, C. M. Cully, V. Angelopoulos, and P. R. Harvey, The electric field instrument (EFI) for THEMIS, *Space Sci. Rev.*, *141*, 303–341, 2008.

Boudouridis, A., H. E. Spence, and T. G. Onsager, Investigation of magnetopause reconnection models using two co-located, low-altitude satellites: A unifying reconnection geometry, *J. Geophys. Res.*, *106*, 29451–29466, 2001.

Chaston, C. C., C. W. Carlson, W. J. Peria, R. E. Ergun, and J. P. McFadden, FAST observation of inertial Alfvén waves in the dayside aurora, *Geophys. Res. Lett.*, *26*, 647, 1999.

Chaston, C. C., L. M. Peticolas, J. W. Bonnell, C. W. Carlson, R. E. Ergun, J. P. McFadden, and R. J. Strangeway, Width and brightness of auroral arcs drven by inertial Alfvén waves, *J. Geophys. Res.*, *108*, doi:10.1029/2001JA007537, 2003.

Chaston, C. C., V. Genot, J. W. Bonnell, C. W. Carlson, J. P. McFadden, R. E. Ergun, R. J. Strangeway, E. J. Lund, and K. J. Hwang, Ionospheric erosion by Alfvén waves, *J. Geophys. Res.*, *111*, doi:10.1029/2005JA011367, 2006.

Chaston, C. C., C. W. Carlson, J. P. McFadden, R. E. Ergun, and R. J. Strangewayg, How important are dispersive Alfvén waves for auroral particle acceleration?, *Geophys. Res. Lett.*, *34*, L07101, doi:10.1029/2006GL029144, 2007.

Connor, H. J., J. Raeder, and K. J. Trattner, Modeling of cusp ion structures and comparison with satellite observations, *J. Geophys. Res.*, *117*, A04203, 2012.

Cully, C. M., R. E. Ergun, K. Stevens, A. Nammari, and J. Westfall, The themis digital fields board, *Space Sci. Rev.*, *141*, 343–355, 2008.

Dombrowski, M. P., J. LaBelle, D. E. Rowland, R. F. Pfaff, and C. A. Kletzing, Interpretation of vector electric field measurements of bursty langmuir waves in the cusp, *J. Geophys. Res*, *117*, A9209, 2012.

Dungey, J. W., The structure of the ionosphere, or adventures in velocity space, in *Geophysics: The Earth's Environment*, edited by C. DeWitt, J. Hieblot, and A. Lebeau, p. 526, Gordon and Breach, New York, 1963.

Escoubet, C. P., M. F. Smith, S. F. Fung, P. C. Anderson, R. A. Hoffman, E. M. Basinska, and J. M. Bosqued, Staircase ion signature in the polar cusp; A case study, *Geophys. Res. Lett.*, *19*, 1735, 1992.

Escoubet, C. P., J. M. Bosqued, J. Berchem, K. J. Trattner, M. G. G. T. Taylor, F. Pitout, H. Laakso, A. Masson, M. Dunlop, H. Reme, I. Dandouras, and A. Fazakerley, You have full text access to this content temporal evolution of a staircase ion signature observed by cluster in the mid-altitude polar cusp, *Geophys. Res. Lett.*, *33*(71), 1735, 2006.

Farrugia, C. J., P. E. Sandholt, W. F. Denig, and R. B. Torbert, Observation of a correspondence between poleward moving auroral formas snd stepped cups ion precipitation, *J. Geophys. Res.*, *103*, 9309, 1998.

Fasel, G. J., Dayside poleward moving auroral forms: A statistical study, *J. Geophys. Res.*, *100*, 891, 1995.

Fasel, G. J., L. C. Lee, and R. W. Smith, Dayside poleward moving auroral forms: A brief review, in *Physics of the Magnetopause*, edited by P. Song and and M. Thomsen B. Sonnerup, volume 90 of *Geophys Monogr. Ser.*, p. 439–447, Washinton, D.C., 1995. AGU.

Fuselier, S. A., J. Berchem, K. J. Trattner, and R. Friedel, Tracing ions in the cusp and low-latitude boundary layer using multispacecraft observations and a global mhd simulation, *J. Geophys. Res.*, *107(A9)*, 1226, 2002a.

Fuselier, S. A., H. U. Frey, K. J. Trattner, S. B. Mende, and J. L. Burch, Cusp aurora dependence on interplanetary magnetic field Bz, *J. Geophys. Res.*, *107(A7)*, 1111, 2002b.

Fuselier, S. A., S. B. Mende, T. E. Moore, H. U. Frey, S. M. Petrinec, E. S. Claflin, and M. R. Collier, Cusp dynamics and ionospheric outflow, in *Magnetospheric ImagingThe Image Mission*, edited by J. L. Burch, volume 109, p. 285, 2003.

Jacobsen, K. S., A. Pedersen, J. I. Moen, and T. A. Bekkeng, A new langmuir probe concept for rapid sampling of space plasma electron density, *Meas. Sci. Technol.*, *21*, 2010.

Kintner, P. M., J. Bonnell, S. Powell, J.-E. Wahund, and B. Holback, First results from the freja HF snapshot receiver, *Geophys. Res. Lett.*, *22*, 287, 1995.

Kintner, P. M., J. Bonnell, R. Arnoldy, K. Lynch, C. Pollack, and T. Moore, SCIFER - transverse ion acceleration and plasma waves, *Geophys. Res. Lett.*, *23*, 1873, 1996.

Kletzing, C. A., F. S. Mozer, and R. B. Torbert, Electron temperature and density at high latitude, *J. Geophys. Res.*, *103*, 14837, 1998.

LaBelle, J., I. H. Cairns, and C. A. Kletzing, Electric field statistics and modulation characteristics of bursty langmuir waves observed in the cusp, *J. Geophys. Res.*, *in press*, 2010.

Li, B., I. H. Cairns, P. A. Robinson, J. LaBelle, and C. A. Kletzing, Waveform and envelope field statistics for waves with stochastically-driven amplitudes, *Phys. Plasma*, *17*, 032110, doi:10.1063/1.3353092, 2010.

Lockwood, M., and M. F. Smith, Low altitude signatures of the cusp and flux tranfer events, *Geophys. Res. Lett.*, *16*, 879, 1989.

Lockwood, M., and M. F. Smith, The variation of reconnection rate at the dayside magnetopause and cups ion precipitation, *J. Geophys. Res.*, *97*, 14841, 1992.

Lockwood, M., and M. F. Smith, Low- and mid-altitude cups particle signatures for general magnetopause reconnection rate variations, 1. Theory, *J. Geophys. Res.*, *99*, 8581, 1994.

Lockwood, M., S. E. Milan, T. Onsager, C. H. Perry, J. D. Scudder, C. T. Russell, and M. J. Brittnacher, Cusp ion steps, field-aligned currents and poleward moving auroral forms, *J. Geophys. Res.*, *106*, 29555, 2001.

Lorentzen, D. A., C. S. Deere, J. I. Minow, R. W. Smith, H. C. Stenbaek-Nielsen, F. Sigernes, R. Arnoldy, and K. Lynch, SCIFER - dayside auroral signatures of magnetospheric energetic electrons, *Geophys. Res. Lett.*, *23*, 1885, 1996.

McAdams, K. L., J. LaBelle, P. Schuck, and P. M. Kintner, PHAZE II observations of lower hybrid burst structures occuring on density gradients, *Geophys. Res. Lett.*, *25*, 3091, 1998.

Milan, S. E., M. Lester, S. W. H. Cowley, and M. Brittnacher, Convection and auroral response to a southward turning of the IMF: Polar UVI, CUTLASS, and IMAGE signatures of transient magnetic flux transfer at the magnetopause, *J. Geophys. Res.*, *105*, 15755, 2000.

Moen, J. I., K. Oksavik, T. Abe, M. Lester, Y. Saito, T. A. Bekkeng, and K. S. Jacobsen, First in-situ measurements of hf radar echoing targets, *Geophys. Res. Lett.*, 2012.

Newell, P. T., and Ching-I. Meng, Ion acceleration at the equatorward edge of the cusp: Low altitude

observations of patch merging, *Geophys. Res. Lett.*, *18*, 1829, 1991.

Onsager, T. G., C. A. Kletzing, J. B. Austin, and H. MacKiernan, Model of magnetosheath plasma in the magnetosphere: Cusp and mantle precipitation at low altitudes, *Geophys. Res. Lett*, *20*, 479, 1993.

Onsager, T. G., S.-W. Chang, J. D. Perez, J. B. Austin, and L. X. Janoo, Low-altitude observations and modeling of quasi-steady magnetopause reconnection, *J. Geophys. Res.*, *100*, 11831, 1995.

Peterson, W. K., Y.-K. Tung, W. J. Burke, C.W. Carlson, J. H. Clemmons, H. L. Carlson, R. E. Ergun, S. A. Fuselier, C. A. Kletzing, D. M. Klumpar, O. W. Lennartsson, R. P. Lepping, N. C. Maynard, J. P. McFadden, T. O. Onsager, W. J. Peria, C. T. Russell, E. G. Shelley, L. Tang, and J. Wygant, Simultaneous observations of solar wind plasma injection from fast an polar, *Geophys. Res. Lett.*, *25*, 2081, 1998.

Pfaff, R., J. Clemmons, C. Carlson, R. Ergun, J. McFadden, F. Mozer, M. Temerin, D. Klumpar, W. Peterson, E. Shelley, E. Moebius, L. Kistler, R. Strangeway, R. Elphic, and C. Cattell, Initial FAST observations of acceleration processes in the cusp, *Geophys. Res. Lett.*, *25*, 2037, 1998.

Phan, T., L. Kistler, B. Klecker, G. Haerendel, G. Paschmann, B. Sonnerup, W. Baumjohann, M. Bavassano-Cattaneo, C. Carlson, A. DiLellis, K.-H. Fornacon, L. Frank, M. Fujimoto, E. Georgescu, S. Kokubun, E. Moebius, T. Mukai, and M. Ieroset, Extended magnetic reconnection at the earth's magnetopause from detection of bi-directional jets, *Nature*, *404*, 848, 2000.

Pottelette, R., and R. Treumann, Impulsive broadband electrostatic noise in the cleft: a signature of dayside reconnection, *J. Geophys. Res.*, *103*, 9299, 1998.

Pottelette, R., M. Malingre, N. Dubouloz, B. Aparicio, R. Lundin, G. Holmgren, and G. Marklund, High frequency waves in the cusp/cleft region, *J. Geophys. Res.*, *95*, 5957, 1990.

Sandholt, P. E., W. F. Denig, C. J. Farrugia, Bjorn Lybek, and Espen Trondsen, Auroral structure at the cusp equatorward boundary: Relationship with the electron edge of low-latitude boundary layer precipitation, *J. Geophys. Res.*, *107*, doi:10.1029/2001JA005081, 2002.

Sauer, K., and R. Sydora, Langmuir-whistler oscillitons and its relation to auroral hiss, *Ann. Geophys.*, *29*, 1–15, 2011.

Sauer, K., and R. Sydora, Mode crossing effects at electron beam-plasma interaction and related phenomena, *Plasma Phys. Control. Fusion*, *54*, 124045, 2012.

Smith, M. F., and M. Lockwood, Earth's magnetospheric cusps, *Rev. Geophys.*, *34*, 233, 1996.

Stasiewicz, K., B. Holback, V. Krasnoselskikh, M. Boehm, R. Boström, and P. M. Kintner, Parametric instabilities of Langmuir waves observed by Freja, *J. Geophys. Res.*, *101*, 21515, 1996.

Stauning, P., F. Primdahl, J. Watermann, and O. Rasmussen, IMF B_y-related cusp currents observed from the oersted satellite and from the ground, *J. Geophys. Res.*, *28*, 99, 2001.

Strangeway, R. J., C. T. Russell, C. W. Carlson, J. P. McFadden, R. E. Ergun, M. Temerin, D. M. Klumpar, W. K. Peterson, and T. E. Moore, Cusp field-aligned currents and ion outflows, *J. Geophys. Res.*, *105*, 21129, 2000.

Strangeway, R. J., R. E. Ergun, Y.-J. Su, C. W. Carlson, and R. C. Elphic, Cfactors controlling ionospheric outflows as observed at intermediate altitudes, *J. Geophys. Res.*, *110*, A03221, 2005.

Su, Y.-J., S. T. Jones, R. E. Ergun, and S. E. Parkery, Modeling of field-aligned electron bursts by dispersive alfvén waves in the dayside auroral regions, *J. Geophys. Res.*, *109*, A11201, 2001.

Tanaka, H., Y. Saito, K. Asamura, S. Ishii, and T. Mukai, High time resolution measurement of multiple electron precipitations with energy-time dispersion in high-latitude part of the cusp region, *J. Geophys. Res.*, *110*, A07204, doi:10.1029/2004JA010664, 2005.

Taylor, E., P. Harvey, M. Ludlam, P. Berg, R. Abiad, and D. Gordon, Instrument data processing unit for THEMIS, *Space Sci. Rev.*, *141*, 153–169, 2008.

Trattner, K. J., S. A. Fuselier, W. K. Peterson, J. A. Sauvaud, H. Stenuit, and N. Dubouloz, On spatial and temporal signatures in the cusp, *J. Geophys. Res.*, *104*, 28411, 1999.

Trattner, K. J., S. A. Fuselier, W. K. Peterson, M. Boehm, D. Klumpar, C. W. Carlson, and T. K. Yeoman, Temporal versus spatial interpretation of cusp ion structures observed by two spacecraft, *J. Geophys. Res.*, *107*, doi:10.1029/2001JA000181, 2002.

Trattner, K. J., S.A. Fuselier, T.K. Yeoman, A. Korth, M. Fraenz, C. Mouikis, H. Kucharek, L.M. Kistler, C.P. Escoubet, H. Reme, I. Dandouras, J.A. Sauvaud, J.M. Bosqued, B. Klecker, C. Carlson, T. Phan, J.P. McFadden, E. Amata, and L. Eliasson, Cusp structures: Combining multi-spacecraft observations with ground based observations, *Ann. Geophys.*, *21*, 2031–2041, 2003.

Trattner, K. J., S.A. Fuselier, S.M. Petrinec, T.K. Yeoman, C. Mouikis, H. Kucharek, and H. Reme, Reconnection sites of spatial cusp structures, *J. Geophys. Res.*, *110*, A04207, doi:10.1029/2004JA010722, 2005a.

Trattner, K. J., S.A. Fuselier, T.K. Yeoman, C. Carlson, W.K. Peterson, A. Korth, H. Reme, J.A. Sauvaud, and N. Dubouloz, Spatial and temporal cusp structures observed by multiple spacecraft and ground observations, in *Surveys in Geophysics*, edited by T.A. Fritz and S.F. Fung, volume 26, p. 281–305. Springer Science and Business Media B.V, 2005b.

Trattner, K. J., J.S. Mulcock, S.M. Petrinec, and S.A. Fuselier, Probing the boundary between anti-parallel and component reconnection during southwards interplanetary magnetic field conditions, *J. Geophys. Res.*, *112*, A08210, 2007.

Trattner, K. J., S.A. Fuselier, S.M. Petrinec, T.K. Yeoman, C.P. Escoubet, and H. Reme, The reconnection site of temporal cusp structures, *J. Geophys. Res.*, *113*, A07S14, doi:10.1029/2007JA012776, 2008.

Yeoman, T. K., M. Lester, S. W. H. Cowley, S. E. Milan, J. Moen, and P. E. Sandholt, Simultaneous observatons of the cups in optical, dmsp, and hf radar data, *Geophys. Res. Lett.*, *24*, 2251, 1997.